Andrzej GAŁECKI, Marek MICHALCZUK, Arkadiusz KASZEWSKI, Bartłomiej UFNALSKI, Lech M. GRZESIAK

Institute of Control and Industrial Electronics, Warsaw University of Technology

doi:10.15199/48.2018.06.08

Particle swarm optimization of the multioscillatory LQR for a three-phase grid-tie converter

Abstract. *This paper presents an evolutionary optimization of the linear-quadratic (LQ) current controller for a three-phase grid-tie voltage source converter with an L-type input filter. The current control system is equipped with multi-oscillatory terms, which enable the converter to obtain nearly sinusoidal shape and balanced input currents under unbalanced and distorted grid voltage conditions. The augmentation of the state vector to include additional states which describe dynamics of disturbances increases the number of weights to be selected for a cost function in the LQR procedure design. Therefore, it is proposed that optimal weighting factors are sought using particle-swarm-based method. Finally, the simulational tuning based on the linear model and the numerical verification based on a non-linear model of the system with a pulse width modulator are addressed.*

Streszczenie. *Artykuł prezentuje optymalizację ewolucyjną liniowo-kwadratowego regulatora prądu dla trójfazowego przekształtnika sieciowego z filtrem wejściowym typu L. Układ regulacji prądu jest wypozażony w człony oscylacyjne co pozwala na kształtowanie niemal sinusoidalnych i symetrycznych prądów wejściowych w warunkach występowania wyższych harmonicznych i asymetrii napięć sieci. Rozszerzenie wektora stanu o dodatkowe stany opisujące dynamikę zakłóceń zwiększa liczbę wag, które należy dobrać dla funkcji celu ujętej w procedurze projektowania LQR. Dlatego zaproponowano dobór optymalnych wsółczynników wagowych przy użyciu optymalizacji metodą roju cząstek. Finalnie zostały omówione strojenie symulacyjne na modelu liniowym oraz weryfikacja numeryczna na modelu nieliniowym z modulatorem szerokości impulsów.* ***(Optymalizacja rojem cząstek regulatora liniowo-kwadratowego z członami oscylacyjnymi dla trójfazowego przekształtnika sieciowego)***

Keywords: grid-side converter, linear-quadratic regulator, current controller, particle swarm optimization, power quality
Słowa kluczowe: przekształtnik sieciowy, regulator liniowo-kwadratowy, regulator prądu, optymalizacja rojem cząstek, jakość energii

Introduction

The LQR design method is known to deliver good performance, therefore is widely employed for developing control systems for voltage source converters. The procedure requires prior preparation of a state-space description of a system and setting weighting matrices employed to solve optimization problem to minimize the quadratic cost function. Selecting the state and input weighting matrices (Q and R) is a crucial stage. Commonly, trial and error approach based on the designer's experience is employed for this part of the LQR procedure, which not only burdens the design but also results in non-optimal response according to commonly used control performance indices such as the integral of squared error or the integral of generalized squared error. Hence, in this paper the LQ current controller design procedure for grid-tie converter is enhanced by using particle swarm optimization algorithm (PSO) to find weighting matrices.

In literature, the multi-variable control systems for grid-tie converters have been designed based on state-space approach e.g by using a zero-pole analysis [1, 2] or by formulating a convex optimization problems in terms of a linear matrix inequality (LMI) constrains and solved using computational packages such as SeDuMi for MATLAB® [3, 4, 5]. In addition to the above solutions, this design problem can be solved using trajectory-based metaheuristic methods or population-based metaheuristic methods like genetic algorithm (GA) [6] or PSO. The PSO technique for partially automated optimizing the controller parameters has been developed for voltage source inverter with LC output filter [7] or multi-modular converters [8]. A review and a classification of meta-heuristic optimization strategies for power converters have been presented in [9]. It should be added here, that the Naslin polynomial method for a state feedback controller design including more than one oscillatory terms yields the problem of contradictory equations. An extensive explanation is given in [10].

The purpose of this paper is to present in details the procedure of designing the multi-oscillatory LQ current controller for grid-tie converter. The novelty introduced in the paper is the usage of PSO for selecting the weighting matrices (Q and R). Comparison of the effectiveness of the proposed optimization method with other methods is out of the paper. The evolutionary optimization of a state feedback current controller with oscillatory terms for a three–phase grid–tie voltage source converter (VSC) operating under distorted grid voltage conditions has been considered in relation to the physical 250 kVA superconducting magnetic energy storage (SMES) [11, 12] system which is currently under construction. The power electronics interface of the SMES system is conceptually shown in Fig. 1 and referred in the literature as the VSC–based SMES.

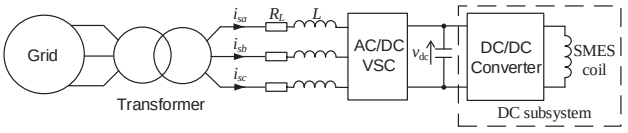

Fig. 1. Block diagram of the SMES system connected to the grid using grid-tie converter

The control strategy of the grid–tie VSC has been developed based on the voltage oriented control (VOC) method [13], where a linear–quadratic (LQ) current control [14] with oscillatory terms based on second order generalized integrator (SOGI) [15] structure has been used.

System description

The designed control system of the grid–side VSC is presented in Fig. 2. The scaling gains k_i and k_{dc} are used to obtain a per–unit control system.

In the outer control loop, a proportional–integral DC–link voltage controller with the anti–windup mechanism based on an integrator clamping [16] is used. The tuning method using the Naslin polynomial approach [17] applied for the PI controller of the DC–link voltage is given in the previous work [18]. The 100 Hz notch filter ($\mathrm{NF}_{2\omega}$) is used to attenuate interference of double grid frequency in case of operating under unbalanced grid voltage conditions. Due to the fact that the DC–link voltage signal has higher harmonics and measurement noise the low–pass filter (LPF) is used.

In the inner control loop, the LQ state–feedback current controller with the anti–windup mechanism has been designed in a positive–sequence rotating reference frame (RRF). In order to track the angle θ of the grid voltage space

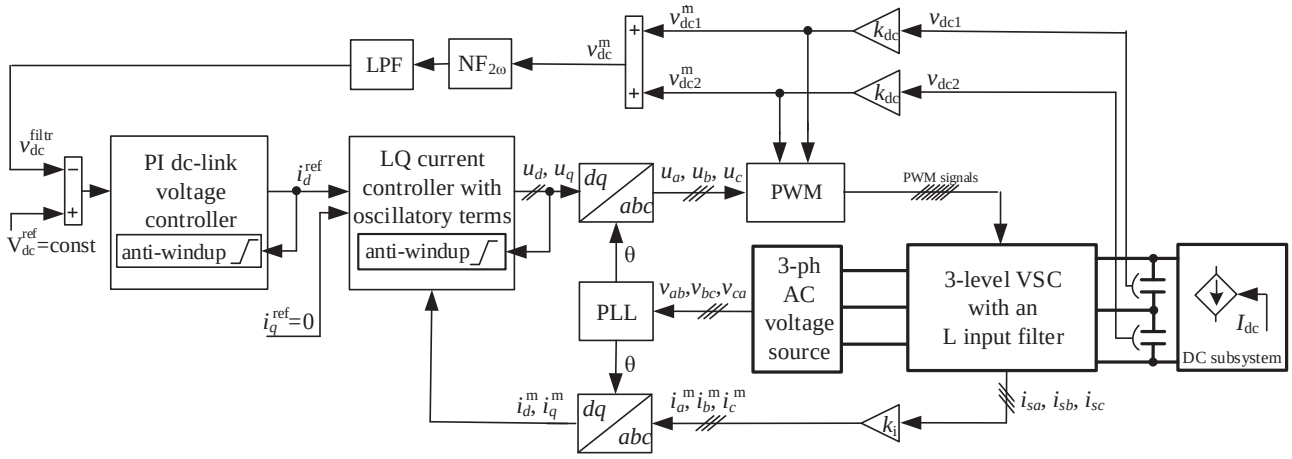

Fig. 2. Block diagram of the grid converter control

vector a phase–locked loop (PLL) based on delayed signal cancellation method [19] is applied. The current controller is equipped with oscillatory terms, which enables the converter to obtain nearly sinusoidal shape and balanced input currents under unbalanced and distorted grid voltage conditions. The anti–windup strategy for the current controller is a combination of two mechanisms. In the proportional–integral part, the integrator clamping method is used. In the oscillatory part, the strategy based on adjusting the damping factor ζ of a damped oscillatory terms has been applied as presented in [20, 21]. Therefore, the details of this issue have been omitted here.

In order to ensure a maximum linear range a pulse–width modulation with triplen harmonic zero–sequence signal (TH–ZSS–PWM) is used. The length of the control signal vector is located up to $\mathrm{U_{max}} = 2/\sqrt{3} \cong 1.1547$.

In the developed numerical models, the power grid has been modeled as a three-phase voltage source, where a few percent unbalance and selected odd harmonics contribution (5th – 6%, 7th – 5%) have been applied. Moreover, the DC subsystem (DC/DC converter and SMES coil in the physical system) is modeled as a current controlled current source, where $\mathrm{I_{dc}}$ is the nominal DC subsystem current.

LQ current controller design

For the purposes of current controller design the state-space model is obtained using small-signal average technique. Assuming that v_{dc} is $V_{\mathrm{dc}} = \mathrm{const.}$ and $\omega = \mathrm{const.}$ the linear state-space model in the dq rotating reference frame is presented as follows:

$$\frac{\mathrm{d}}{\mathrm{d}t}\mathbf{x} = \mathbf{A}\mathbf{x} + \mathbf{B}\mathbf{u} + \mathbf{E}\mathbf{v} \ , \tag{1a}$$

where

$$\mathbf{A} = \begin{bmatrix} -\frac{R_L}{L} & \omega \\ -\omega & -\frac{R_L}{L} \end{bmatrix}, \ \mathbf{x} = \begin{bmatrix} i_d^{\mathrm{m}} \\ i_q^{\mathrm{m}} \end{bmatrix} \ , \tag{1b}$$

$$\mathbf{B} = \begin{bmatrix} -\frac{V_{\mathrm{dc}}}{L}k_i & 0 \\ 0 & -\frac{V_{\mathrm{dc}}}{L}k_i \end{bmatrix}, \ \mathbf{u} = \begin{bmatrix} u_d \\ u_q \end{bmatrix} \ , \tag{1c}$$

$$\mathbf{E} = \begin{bmatrix} \frac{1}{L}k_i & 0 \\ 0 & \frac{1}{L}k_i \end{bmatrix}, \ \mathbf{v} = \begin{bmatrix} v_d \\ v_q \end{bmatrix} \ . \tag{1d}$$

There are two state signals i_d^{m} and i_q^{m} collected in the state vector $\mathbf{x}$, two control signals u_d and u_q collected in the control vector $\mathbf{u}$ and two disturbance signals v_d and v_q collected in the disturbance vector $\mathbf{v}$. There are also three matrices: $\mathbf{A}$ – the state matrix, $\mathbf{B}$ – the control matrix and $\mathbf{E}$ – the disturbance matrix. The output equation is defined as follows: $\mathbf{y} = \mathbf{C}\mathbf{x} + \mathbf{D}\mathbf{u}$, where $\mathbf{C} = \mathbf{I}_{2x2}$ and $\mathbf{D} = \mathbf{0}_{2x2}$.

In order to provide zero steady–state tracking errors $e_d = i_d^{\mathrm{ref}} - i_d^{\mathrm{m}}$ and $e_q = i_q^{\mathrm{ref}} - i_q^{\mathrm{m}}$ for step type reference signal changes the current control is extended by integral terms trough the introduction of the two variables p_{d} and p_{q} in accordance with:

$$\frac{\mathrm{d}}{\mathrm{d}t}p_x = e_x \ , \tag{2}$$

where subscript $x = \{d, q\}$.

Similarly, in order to reduce the sinusoidal component of the error in the current tracking caused by the voltage distortion, the oscillatory terms are incorporated. They can be described as:

$$\frac{\mathrm{d}}{\mathrm{d}t}r_{1x}^{(h)} = r_{2x}^{(h)} \ , \tag{3a}$$

$$\frac{\mathrm{d}}{\mathrm{d}t}r_{2x}^{(h)} = e_x - (h\omega)^2 r_{1x}^{(h)} - 2\zeta h\omega r_{2x}^{(h)} \ , \tag{3b}$$

where subscript $x = \{d, q\}$ and $h = \{2, 6\}$ denote a selected harmonic order and ζ is a damping factor set at the same level for all selected oscillatory terms [22]. The compensation of the second and the sixth harmonic of the grid currents represented in the d,q frame results in the compensation of unbalance and the fifth and the seventh harmonic in the natural frame [18]. In order to convert the control system from the continuous to the discrete domain, the Tustin approximation with pre–warping is used.

The augmented state–space model in the synchronously RRF is given as follows:

$$\frac{\mathrm{d}}{\mathrm{d}t}\mathbf{x}_{\mathrm{aug}} = \mathbf{A}_{\mathrm{aug}}\mathbf{x}_{\mathrm{aug}} + \mathbf{B}_{\mathrm{aug}}\mathbf{u} + \mathbf{E}_{\mathrm{aug}}\mathbf{v} \ , \tag{4a}$$

where

$$\mathbf{A}_{\mathrm{aug}} = \begin{bmatrix} \mathbf{A_0} & \mathbf{0}_{4x4} & \mathbf{0}_{4x4} \\ \mathbf{A_I} & \mathbf{A}_{(2)} & \mathbf{0}_{4x4} \\ \mathbf{A_I} & \mathbf{0}_{4x4} & \mathbf{A}_{(6)} \end{bmatrix}, \ \mathbf{x}_{\mathrm{aug}} = \begin{bmatrix} \mathbf{x} \\ \mathbf{p} \\ \mathbf{r}_{(2)} \\ \mathbf{r}_{(6)} \end{bmatrix} , \tag{4b}$$

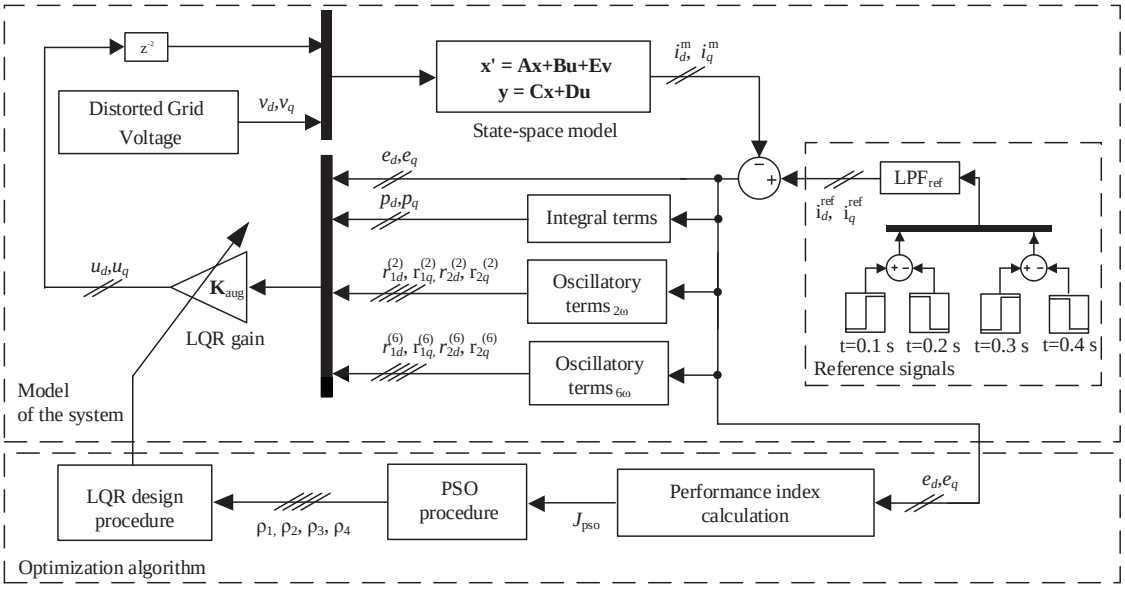

Fig. 3. PSO connected to the numerical model of the system

(4c) $$\mathbf{B}_{\mathrm{aug}} = \begin{bmatrix} \mathbf{B} \\ \mathbf{0}_{10x2} \end{bmatrix}, \mathbf{E}_{\mathrm{aug}} = \begin{bmatrix} \mathbf{E} \\ \mathbf{0}_{10x2} \end{bmatrix},$$

given that

(4d) $$\mathbf{A_0} = \begin{bmatrix} \mathbf{A} & \mathbf{0}_{2x2} \\ \mathbf{I}_{2x2} & \mathbf{0}_{2x2} \end{bmatrix}, \mathbf{A_I} = \begin{bmatrix} \mathbf{0}_{2x2} & \mathbf{0}_{2x2} \\ \mathbf{I}_{2x2} & \mathbf{0}_{2x2} \end{bmatrix},$$

(4e)
$$\mathbf{A}_{(h)} = \begin{bmatrix} \mathbf{0}_{2x2} & \mathbf{I}_{2x2} \\ \mathbf{W}_{(h)} & \mathbf{0}_{2x2} \end{bmatrix}, \mathbf{W}_{(h)} = -\mathtt{diag}([(h\omega)^2, (h\omega)^2])$$

and

(4f) $$\mathbf{p} = [p_d,\ p_q]^{\mathrm{T}},\ \mathbf{r}_{(h)} = [r_{1d}^{(h)}, r_{1q}^{(h)}, r_{2d}^{(h)}, r_{2q}^{(h)}]^{\mathrm{T}}$$

for h={2,6}. In the equations (4a–4b): $\mathbf{A}_{\mathrm{aug}}$ – the augmented state matrix; $\mathbf{B}_{\mathrm{aug}}$ – the augmented control matrix; $\mathbf{E}_{\mathrm{aug}}$ – the augmented disturbance matrix; $\mathbf{x}_{\mathrm{aug}}$ – the augmented state vector;

In order to calculate the full state–feedback current controller gains collected in the matrix $\mathbf{K}_{\mathrm{aug}}$, the LQ method is chosen. The `lqrd` MATLAB®'s function is used, where the state–feedback law $\mathbf{u}(k) = -\mathbf{K}_{\mathrm{aug}}\mathbf{x}_{\mathrm{aug}}(k)$ minimizes the discrete cost function equivalent to the continuous one:

(5) $$J = \int_0^\infty \mathbf{x}_{\mathrm{aug}}^{\mathrm{T}}\mathbf{Q}_{\mathrm{aug}}\mathbf{x}_{\mathrm{aug}} + \mathbf{u}^{\mathrm{T}}\mathbf{R}\mathbf{u}\mathrm{d}t,$$

where $\mathbf{Q}_{\mathrm{aug}} = \mathtt{diag}([\mathbf{Q}, \mathbf{Q_p}, \mathbf{Q_r}])$ and $\mathbf{R} = \mathtt{diag}([r, r])$, are weighting matrices.

It was assumed, that the same penalty weights are applied in both axes d and q of the current control structure. Accordingly, weighting matrices are presented as follows: $\mathbf{Q} = \mathtt{diag}([q, q])$, $\mathbf{Q_p} = \mathtt{diag}([q_p, q_p])$ and $\mathbf{Q_r} = \mathtt{diag}(\mathbf{Q}_{(2)}, \mathbf{Q}_{(6)})$ and where $\mathbf{Q}_{(h)} = \mathtt{diag}([q_r^{(h)}, q_r^{(h)}, \frac{q_r^{(h)}}{(h\omega)^2}, \frac{q_r^{(h)}}{(h\omega)^2}])$ for $h = \{2, 6\}$.

Particle Swarm Optimization of the LQ current controller

In order to find $\mathbf{Q}$ entries the particle swarm optimization (PSO) has been applied as presented in Fig. 3 using the linear model of the system (V_{dc}=const. and $\zeta = 0$).

Four values ρ_i are sought in the optimization process, and they correspond with $\mathbf{Q}$ entries as follows: $q = 10^{\rho_1}$, $q_p = 10^{\rho_2}$, $q_r^{(2)} = 10^{\rho_3}$, $q_r^{(6)} = 10^{\rho_4}$ as presented in Fig. 4 and Fig. 6. As it is stated in [7] introducing the decisive variables as the powers of 10 in the case of selection of Q matrix is more effective than the search in a linear scale. The optimizer is searching a solution in four dimensional space. This processes is performed using virtual particles, that travel in the search space. The set of all particles is called a swarm. Position of the particles in the search space represents a candidate solution. Updating of the particle position is done iteratively according to the formulae:

(6) $$\nu_i^j(k+1) = c_1\nu_i^j(k) + c_2r_1(\rho_i^{\mathrm{pbest}} - \rho_i^j(k)) + c_2r_2(\rho_i^{\mathrm{gbest}} - \rho_i^j(k)),$$

(7) $$\rho_i^j(k+1) = \rho_i^j(k) + \nu_i^j(k+1),$$

where i – particle identification number, k – iteration number, ν_i – speed of the i-th particle, ρ_i^{pbest} – the best solution proposed so far by the i-th particle, ρ_i^{gbest} – the best solution proposed so far by the swarm, r_1,r_2,r_3 - random numbers uniformly distributed between 0 and 1, c_1 the exploitative factor, c_2 – the individuality factor, c_3 – the social factor. The c_1, c_2, and c_3 factors have been obtained using the constricted PSO formula [23] and are 0.729, 1.495, and 1.495, respectively, which can be derived using stability analysis provided in [24].

In each iteration candidate solutions represented by position of particles are rated according to the objective function in the simulation test. Pulses of the reference signals i_d^{ref} and i_q^{ref} are formed in the test as depicted in Fig. 7. The selected objective function bases of the integral square error index is given as follows:

(8) $$J_{\mathrm{pso}} = \sum_{k=0}^{N} \mathbf{e}(\mathbf{k})^{\mathrm{T}}\mathbf{e}(\mathbf{k}).$$

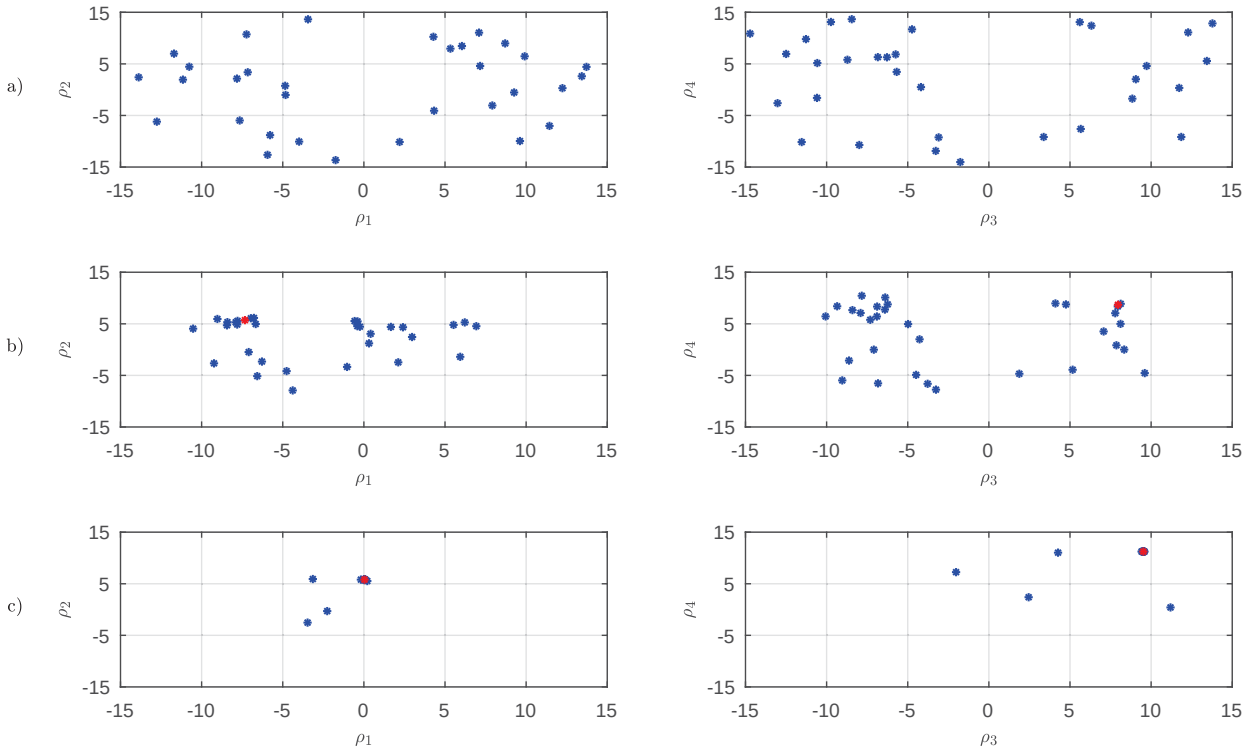

Fig. 4. Initial particles positions (a), positions after the 15th (b) and 100th (c) iteration

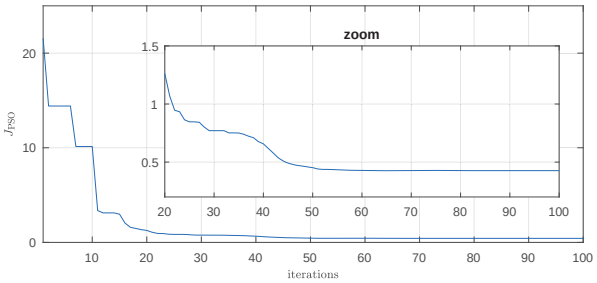

Fig. 5. The evolution of the performance index

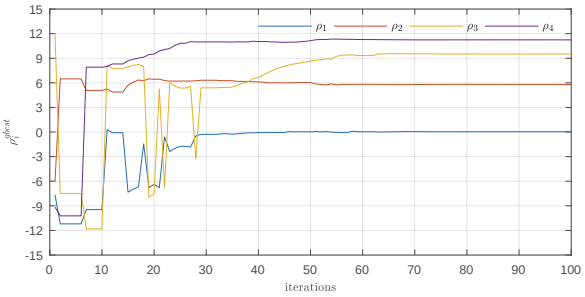

Fig. 6. The best set of parameters ρ_i found during the optimization process

The swarm convergence over the optimization process is shown in Fig. 4. The red marker denotes the best position found so far. The evolution of the performance index J_{pso} for the $qbest$ solution over swarm search iterations is presented Fig. 5. The value of sought parameters proposed by the swarm after each iteration is presented in Fig. 6. The number of executed iterations is 100. The change of the current response for the best so far found solution over the optimization progress is illustrated in Fig 7. Finally, the assumed dynamic performance as well as the ability of rejecting higher harmonics have been met (Fig 7c) after 100 iterations.

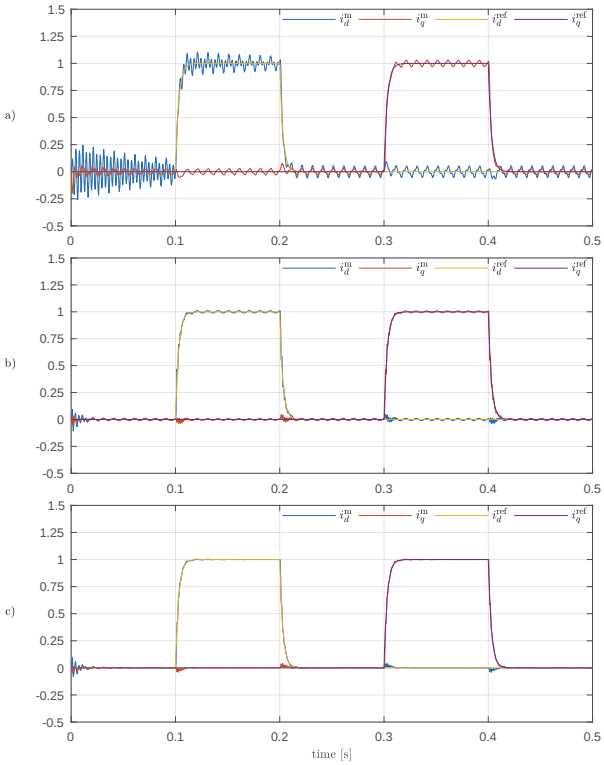

Fig. 7. The i_d^{m} and i_q^{m} current components in the simulation test for the best solution after 10th (a), 30th (b) and 100th (c) iteration

It should be kept in mind that the optimizer has a full access to $\mathbf{Q}$, so it is searching the solution without paying attention to the control effort. However, if the control effort is neglected in the optimization, the found solution may turn out to be unstable in a real system because of unavoidable identification errors and noise in the measurements signal.

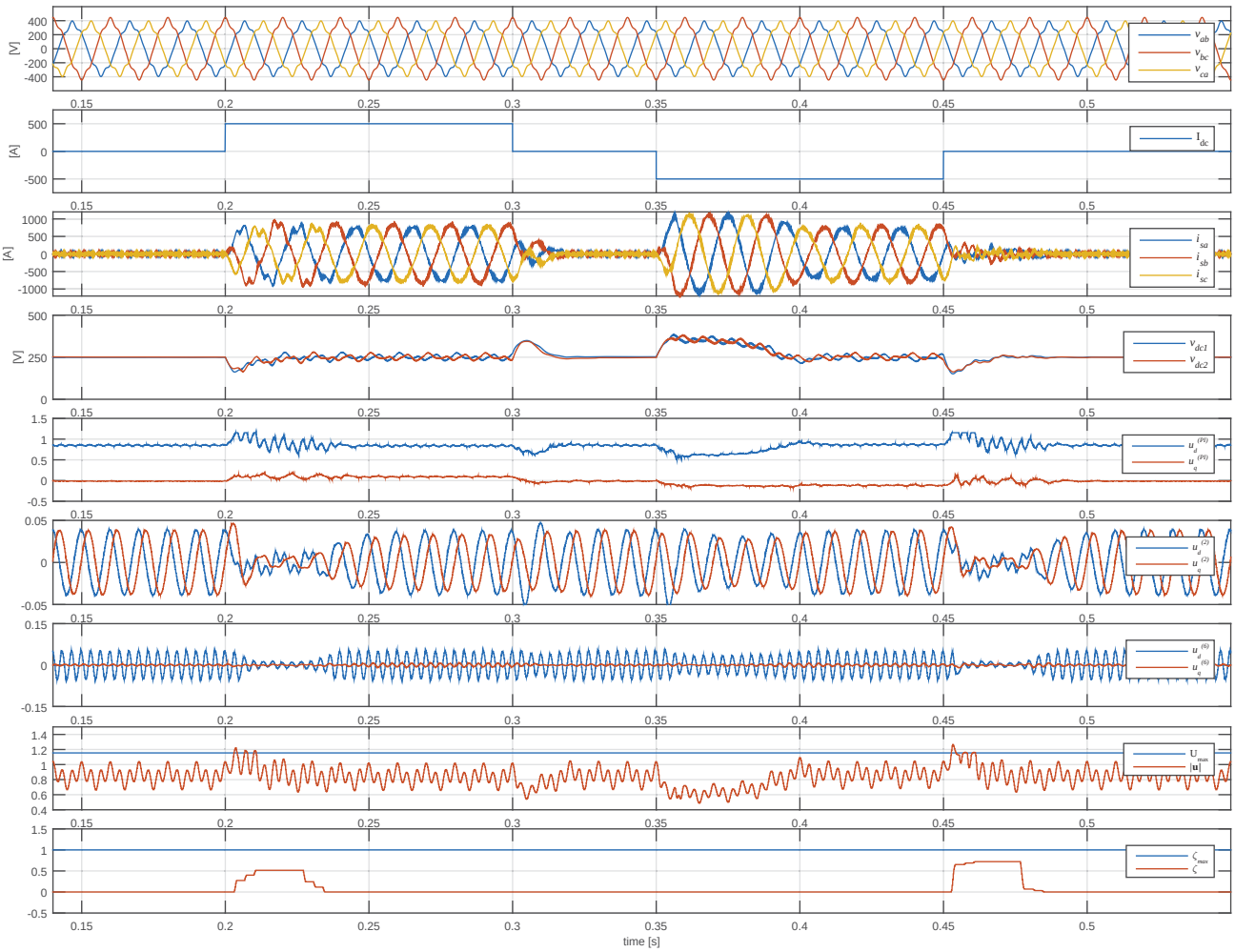

Fig. 8. Performance of the LQ current control system tuned by PSO

Some restriction on the control signal in the dynamic state are required. It can be performed in many ways. In the study presented in [7] the penalty function has been added to the objective function. This methods comes with a drawback, because the new element in performance index needs a subjective weight that has to be set by guessing and checking. In this study too aggressive control behavior is penalized by reducing the dynamics of the reference signals. The pulses of reference signals (Fig. 7) are generated as a step change filtered by the first order low pass filter $\mathrm{LPF}_{\mathrm{ref}}$. In this method, the desired dynamics of the current control loop is directly defined by reference signal and there is no need to use a combined performance index.

The swarm consists of 32 particles and is initialized with random particle position uniformly distributed in the search space limited from -15 to 15 in all dimensions. Preliminary tests have shown that, due to discretization and delays in the current control loop the exponents for Q entries above 15 result in gains of the feedback controller, that are not possible to be implemented even in the simulation models. Relatively large number of particles in relation to the number of dimensions of the search space results from the vast boundaries of the search space. Because the optimization is performed off-line this parameter is not crucial.

During the optimization process the swarm is gradually converging to the best so far found solution. However, to avoid the getting stuck of the swarm in the local minimum, the convergence should not be unduly fast. Very common practice preventing the swarm from premature convergence is limiting the particle velocity [25, 26]. A simple rule of thumb is to set the maximum velocity at a value equal from 5% to 10% of the range of the search space. In this study the velocity limit is set to 1.

After 100 iterations (Fig. 4c) the $85\,\%$ of all particles are usually in a radius of 0.1 from the global best position, taking into account all dimensions of the search-space. The rest of particles, that are more distant form the best position, are not converging intensively because of long distance between the best global position and the best found so far particle position. It should be noted that very high convergence of the swarm, typical for many PSO applications, is not necessary. The weak convergence of some particles does not affect the quality of the final solution.

Numerical results

A numerical discrete grid-tie converter model has been built according to the scheme from Fig. 2 to verify the proposed current controller synthesis method. The key parameters of the setup are listed in Tab. 1. The behavior of the system under selected load variation is shown in Fig. 8. The energy flow from the grid to the DC subsystem takes place between $0.2\,\mathrm{s}$ and $0.3\,\mathrm{s}$ while from $0.35\,\mathrm{s}$ to $0.45\,\mathrm{s}$ the direction is opposite. In the steady–state, nearly sinusoidal and balanced grid current shape has been obtained. In the transient–state, a fast dynamic response has been provided. Moreover, the adjusting mechanism of the damping factor for the oscillatory terms is applied as well as in [20, 21], result-

ing in almost complete suppression of oscillatory terms in the transient-states linked with the load variation, limiting their influence on the control signals.

Table 1. Selected parameters of the grid–tie converter numerical model

Symbol	Value	Description
$\mathrm{V_{dc}}$	500 V	Nominal DC–link voltage
V	285 V	Nominal input voltage RMS value
ω	100π s^{-1}	Nominal pulsation of the input voltage
L	0.12 mH	Inductances of the input filter
R_{L}	4 mΩ	Resistances of the input filter
C	6.0 mF	Capacitance of the DC–link capacitor
$\mathrm{I_{dc}}$	500 A	Nominal DC subsystem current
$\mathrm{F_s}$	5 kHz	Switching/sampling frequency
$\mathrm{k_{dc}}$	1/500	DC–link voltage scaling factor
$\mathrm{k_i}$	1/1000	Current scaling factor

Conclusions

The novel approach to LQ current controller tuning for a three-phase grid-tie voltage source converter has been proposed and tested numerically. The current controller gains has been determined using LQR design procedure. The weighting matrices for the LQR has been optimized using the PSO method, where parameterless objective function has been proposed. This makes the tuning procedure more straightforward in comparison to the often reported trial-and-error method, where multi-dimensional weights-finding problem must be solved.

The research was partially supported by the National Centre for Research and Development (Narodowe Centrum Badań i Rozwoju) within the project No. PBS3/A4/13/2015 entitled "Superconducting magnetic energy storage with a power electronic interface for the electric power systems" (original title: "Nadprzewodzący magazyn energii z interfejsem energoelektronicznym do zastosowań w sieciach dystrybucyjnych"), 01.07.2015–31.12.2018. The acronym for the project is NpME.

***Authors**: Andrzej Gałecki, MSc, Marek Michalczuk, PhD, MSc, Arkadiusz Kaszewski, PhD, MSc, Bartłomiej Ufnalski, PhD, DSc, prof. Lech Grzesiak, PhD, DSc, Institute of Control and Industrial Electronics, Faculty of Electrical Engineering, Warsaw University of Technology, 75 Koszykowa St., Warsaw 00-662, Poland, email: andrzej.galecki@ee.pw.edu.pl*

REFERENCES

[1] J. Dannehl, M. Liserre, F. W. Fuchs.: Filter-based active damping of voltage source converters with LCL filter, IEEE Trans. on Industrial Electronics, 58(8), pp. 3623–3633, 2011.

[2] A. Vidal, F. D. Freijedo, A. G. Yepes, P. Fernandez-Comesana, J. Malvar, Ó. Lopez, and J. Doval-Gandoy.: Assessment and optimization of the transient response of proportional-resonant current controllers for distributed power generation systems, IEEE Trans. on Ind. Electronics, 60(4), pp. 1367–1383, 2013.

[3] L. A. Maccari, J. R. Massing, L. Schuch, C. Rech, H. Pinheiro, R. C. L. F. Oliveira, and V. F. Montagner.: LMI-based control for grid-connected converter with LCL filters under uncertain parameters, IEEE Transactions on Power Electronics, 29(7), pp. 3776–3785, 2014.

[4] G. G. Koch, C. R. D. Osório, J. R. Massing, H. Pinheiro, V. F. Montagner, L. A. Maccari, and R. C. L. F. Oliveira.: Comparison of controllers based on lmis for grid-connected converters, 8th Intern. Symposium on Power Electronics for Distributed Generation Systems (PEDG), Brazil, pp. 1–5, 2017.

[5] C. Olalla, R. Leyva, A. El Aroudi, I. Queinnec.: Robust LQR control for PWM converters: An LMI approach, IEEE Trans. on Industrial Electronics, 56(7), pp. 2548–2558, 2009.

[6] W. Lenwari, M. Sumner, P. Zanchetta.: The use of genetic algorithms for the design of resonant compensators for active filters, IEEE Trans. on Ind. Electr. 56(8), pp. 2852–2861, 2009.

[7] B. Ufnalski, A. Kaszewski, L. M. Grzesiak.: Particle swarm optimization of the multioscillatory LQR for a three-phase four-wire voltage-source inverter with an LC output filter, IEEE Trans. on Industrial Electronics, 62(1), pp. 484–493, 2015.

[8] E. Rakhshani, A. M. Cantarellas, D. Remon, A. Luna, P. Rodriguez.: PSO-based LQR controller for multi modular converters, IEEE ECCE Asia Downunder (ECCE Asia 2013), pp. 1023–1027, 2013.

[9] S. E. De León-Aldaco, H. Calleja, J. Aguayo Alquicira.: Metaheuristic optimization methods applied to power converters: A review, IEEE Transactions on Power Electronics, 30(12), pp. 6791–6803, 2015.

[10] B. Ufnalski.: Naslin polynomial method and multiresonant current controllers? [web page] `http://www.ufnalski.edu.pl/proceedings/misc/Naslin_MOSC_beamer.pdf`, [Accessed on 2 Jan. 2018].

[11] M. H. Ali, B. Wu, R. A. Dougal.: An overview of SMES applications in power and energy systems, IEEE Trans. on Sus. Energy, 1(1), pp. 38–47, 2010.

[12] J. M. Carrasco, L. G. Franquelo, J. T. Bialasiewicz, E. Galvan, R. C. PortilloGuisado, M. A. M. Prats, J. I. Leon, N. Moreno-Alfonso.: Power-electronic systems for the grid integration of renewable energy sources: A survey, IEEE Trans. on Industrial Electronics, 53(4), pp. 1002–1016, 2006.

[13] M. Bobrowska, K. Rafal, H. Milikua, M.P. Kazmierkowski.: Improved voltage oriented control of AC-DC converter under balanced and unbalanced grid voltage dips, Intern. Conf. devoted to 150 Anniversary of Alexander Popov EUROCON'2009, pp. 772–776, Russia, 2009.

[14] B. Kedjar, H.Y. Kanaan, K. Al-Haddad.: Vienna rectifier with power quality added function, IEEE Transactions on Consumer Electronics, 61(8), pp. 3847–3856, 2014.

[15] A. G. Yepes, F. D. Freijedo, Ó. Lopez, J. Doval-Gandoy.: High-performance digital resonant controllers implemented with two integrators, IEEE Transactions on Power Electronics, 26(2), pp. 563–576, 2011.

[16] A. Scottedward Hodel, C. E. Hall.: Variable-structure PID control to prevent integrator windup, IEEE Trans. on Ind. Electronics, 48(2), pp. 442–451, 2001.

[17] Pierre Naslin.: Essentials of optimal control, Boston Technical Publishers, 1968.

[18] A. Galecki, A. Kaszewski, B. Ufnalski, L. M. Grzesiak.: State current controller with oscillatory terms for three-level grid-connected pwm rectifiers under distorted grid voltage conditions, 17th European Conference on Power Electronics and Applications (EPE), pp. 1–10, 2015.

[19] Yi Fei Wang, Yun Wei Li.: Grid synchronization PLL based on cascaded delayed signal cancellation, IEEE Transactions on Power Electronics, 26(7), pp. 1987–1997, 2011.

[20] A. Galecki, L. M. Grzesiak, B. Ufnalski, A. Kaszewski, M. Michalczuk.: Multi–oscillatory current control with anti–windup for grid–connected VSCs operated under distorted grid voltage conditions, 18th European Conf. on Power Electronics and Applications (EPE'17), pp. 1–10, 2017.

[21] A. Galecki, L. Grzesiak, B. Ufnalski, A. Kaszewski, M. Michalczuk.: Anti-windup strategy for an LQ current controller with osc. terms for 3-phase grid-tie VSCs in SMES systems, Power Electronics and Drives, 1(36), pp. 65–81, 2016.

[22] K. Zhou, Y. Yang, F. Blaabjerg, D. Wang.: Optimal selective harmonic control for power harmonics mitigation, IEEE Trans. on Industrial Electronics, 62(2), pp. 1220–1230, 2015.

[23] M. Clerc, J. Kennedy.: The particle swarm - explosion, stability, and convergence in a multidimensional complex space, IEEE Trans. on Evol. Computation, 6(1), pp. 58–73, 2002.

[24] J. Kennedy, R. C. Eberhart.: A discrete binary version of the particle swarm algorithm, 1997 IEEE International Conference on Systems, Man, and Cybernetics. Computational Cybernetics and Simulation, 5(1), pp. 4104–4108, 1997.

[25] S. Cui, D. S. Weile.: Application of a parallel particle swarm optimization scheme to the design of electromagnetic absorbers, IEEE Transactions on Antennas and Propagation, 53(11), pp. 3616–3624, 2005.

[26] J. Hazra, A. K. Sinha.: A multi-objective optimal power flow using particle swarm optimization, European Transactions on Electrical Power, 21(1), pp. 1028–1045, 2011.